Ain Shams Engineering Journal 13 (2022) 101656

Contents lists available at ScienceDirect

Ain Shams Engineering Journal

journal homepage: www.sciencedirect.com

Design and Analysis of a Novel Generalized Continuous Tracking Differentiator

Wameedh Riyadh Abdul-Adheem [a], Ibraheem Kasim Ibraheem [a,b,*], Amjad J. Humaidi [c], Ahmed Alkhayyat [d], Rami A. Maher [e], Ahmed Ibraheem Abdulkareem [c], Ahmad Taher Azar [f,g]

[a] University of Baghdad, College of Engineering, Department of Electrical Engineering, Al-Jadriyah, 10001 Baghdad, Iraq
[b] Department of Computer Engineering Techniques, Al-Rasheed University College, Baghdad 10001, Iraq
[c] University of Technology, Department of Control and Systems Engineering, 10001 Baghdad, Iraq
[d] College of technical engineering, The Islamic University, Najaf, Iraq
[e] Faculty of Engineering, Isra Univ., P.O. Box 33, 11622 Amman, Jordan
[f] College of Computer and Information Sciences, Prince Sultan University, Riyadh 11586, Saudi Arabia
[g] Faculty of Computers and Artificial Intelligence, Benha University, Benha 15311, Egypt

ARTICLE INFO

Article history:
Received 5 May 2019
Revised 30 July 2021
Accepted 23 November 2021
Available online xxxx

Keywords:
Tracking differentiator
Sigmoid function
Peaking phenomenon
Noise
Chattering phenomenon
Signal derivative

ABSTRACT

In this work, an *n*-th order Generalized Tracking Differentiator (GTD) is proposed based on sigmoid function with a continuous structure, including both linear and nonlinear parts, thus increasing the estimation accuracy of the input signal and its derivatives, and overcoming the inherent issues related to the classical Tracking Differentiators (TDs). Then, a 2nd-order version of the proposed GTD is derived and optimized with further improvements which are reflected in the excellent behavior in the time and frequency domains. Moreover, stability analysis using the method of Lyapunov analysis is also investigated and the performance of the GTD is proven in the time and frequency domains and revealed that the proposed GTD considerably reduces the "peaking phenomenon" and "noise" and eliminates the "chattering phenomenon" from the signal derivatives. The excellent results of the proposed GTD are demonstrated through simulations on noise-free and noisy signals and compared with the Robust Exact Uniformly Convergent Arbitrary Order Differentiator (REUCAOD).

1. Introduction

Real-time signals differentiation is a well-understood subject. A perfect differentiator would have to achieve the differentiation to the noise with perhaps a high amplitude of the derivatives as well as the signal itself [1]. Numerous applications call for the inexorableness of the differentiator design, nevertheless, the ideal differentiator cannot be constructed, together with the fundamental signal, it would be required to differentiate the high-frequencies components of the noise which are ingrained in the signal and may possess large values of derivatives [2].

Building a tracking differentiator as a distinct unit is a typical plan goal for the signal processing field. The underlying methodology is to permit a simple dynamic model to characterize the ideal differentiator's transfer function. The disadvantage of this method is that the bandwidth of the signal to be differentiated should be less than the differentiator's bandwidth. Otherwise, the differentiator will not produce a precise differentiation for the signal [2].

Over the past two decades, the high levels of performance demanded from control and navigation systems have initiated numerous innovations in the design of tracking differentiators [3]. Some of these designs, which will be considered in the development of the proposed GTD include A Traditional High-Gain Differentiator (HGTD) [3–5]. A trade-off between the noise tolerance and an error about its non-existence characterizes this system. It enables accurate differentiation when the differentiator gains have very high values (approach infinity), which makes it practically unrealizable. The HGTD can restrain high-frequency noises under certain conditions. A Robust Exact Differentiator (RED) [2], uses a sliding mode technique in its design and, to its disadvantage,

* Corresponding author.
Peer review under responsibility of Ain Shams University.

Production and hosting by Elsevier

https://doi.org/10.1016/j.asej.2021.101656

requires an upper limit for the Lipschitz constant of its derivative. The differentiation suffers from the chattering phenomenon due to the existence of a non-smooth discontinuous function. The RED is desirable in high accuracy systems with a lightly noise-contaminated environment. A Hybrid Continuous Nonlinear Differentiator (HCND) [6], this system has the advantages of enhanced dynamic performance and the capacity to mitigate the chattering phenomenon and noises, due to its continuous structure, which comprises both linear and nonlinear terms. The Rapid Convergent Nonlinear Differentiator (RCND) [7]. While the RCND is not suitable for a delayed signal application, it effectively enhances dynamic performance and inhibits high-frequency noise. Robustness is optimized by the integration of sliding mode items and a linear filter, and the system further mitigates the chattering phenomenon in the output of derivative estimations. The Robust Exact Uniformly Convergent Arbitrary Order Differentiator (REUCAOD) [8], developed from the basis of a High Order Sliding Mode (HOSM) differentiator. This type of tracking differentiator is characterized by two features, namely finite-time accurate convergence, despite the presence of perturbation, and uniform convergence of the initial differentiator errors. The sole condition is that the n-th derivative is uniformly bound by a known constant for a signal to be differentiated $(n-1)$ times. As the HOSM differentiator does not have uniform convergence concerning the initial differentiation errors, the time required for the convergence might grow indefinitely simultaneously with the growth of the initial differentiation error. The latter's trajectories are, therefore, driven independently into a neighboring compact zone using the uniform part, and it is the role of the HOSM differentiator to return the differentiation error to zero within a specified time.

In practice, many applications have been proposed based on TDs to achieve high-performance control, such as an autonomous underwater vehicle (AUV) in the diving plane to control its pitch and depth [9], single-phase active power filters to detect the harmonic currents [10], detection systems of geomagnetic attitude [11], speed control of permanent magnet DC (PMDC) motor [12], dynamic speed control of differential drive mobile robot (DDMR) [13], motion control of Unmanned Aerial Vehicle (UAV) [14]. Moreover, practical interest in system identification is driven by difficulties associated with deriving models from physical principles. Such models are useful for enhancing physical understanding; analyzing system properties; and performing simulation, prediction, filtering, state estimation, monitoring, and fault diagnosis as well as control. This makes the TDs are leading in system identification applications. Finally, an example of the usage of TDs in other engineering disciplines is described in [15]. In [16], a sigmoid function-based augmented nonlinear differentiator was presented. The convergence property was investigated via singular perturbation theory and The robustness performance against noises was analyzed through describing function method. In [17], a higher-order derivative is obtained by connecting the proposed differentiator in series.

In this paper, an n-th order Generalized Tracking Differentiator (GTD) is proposed based on sigmoid function and its convergence is proven using Lyapunov Function. It offers a continuous structure, including both linear and nonlinear terms. Then, a 2nd order version of the proposed tracking differentiator is derived and optimized with further developments which have been reflected in the excellent behavior of the proposed 2nd order GTD in the time and frequency domains. Based on the aforementioned, the GTD overcomes the inherent issues related to the classical TDs.

The main contributions of this paper are twofold. Firstly, an n-th order Generalized Tracking Differentiator (GTD) is proposed based on the sigmoid function to generate an (n-1) derivatives of the signal in noisy and noise-free environments. It offers a continuous structure, including both linear and nonlinear terms. Secondly, the convergence of the GTD is proven using Lyapunov functions and its behavior is analyzed in time and frequency domains, where certain conditions on the parameters of the proposed GTD are derived for optimum differentiation of noisy signals. As far as the authors of this paper know, no structure and convergence analysis similar to what is presented in this paper are found in the literature.

The paper is structured as follows. Section 2 states the problem with this work. A presentation of the proposed GTD and the pertinent stability analysis are investigated in Section 3. The numerical simulations confirming the soundness of the offered configuration are demonstrated in section 4. Finally, the conclusions are mentioned in Section 5.

2. Problem Statement

Generally speaking, the differentiator is an estimator, which is independent of the model. Given a signal $r(t)$ that may be contaminated with noise. Approximately, the differentiator of a certain signal $r(s)$ can be expressed as a linear operator as $\frac{s}{\tau s+1}r(s)$. This approximation is relatively vulnerable to the presence of noise in $r(t)$ because it is strengthened by a factor of $1/\tau$. The real-time tracking dynamic differentiation problem involves finding an estimate of the input signal $r(t)$ and its derivatives up to the (n-1)-*th* order, these estimations are represented as $r_1, r_2, \cdots,$ andr_n , respectively. The dynamics of the *n-th* order nonlinear differentiator is described as:

$$\begin{cases} \dot{r}_1(t) = r_2(t), \\ \dot{r}_2(t) = r_3(t), \\ \quad\vdots \\ \dot{r}_n(t) = f(r_1(t) - r(t), r_2(t), \cdots, r_n(t)). \end{cases} \tag{1}$$

Proposing the nonlinearity f in the structure of the differentiator increases the estimation accuracy of the input signal and its derivatives, but on the other hand, it may introduce several unwanted phenomena such as "chattering phenomenon", "peaking phenomenon", and "noise amplification". It is required to select the special structure of the differentiator that includes some type of nonlinearities to overcome such difficulties. Moreover, the stability of the differentiator in the sense that $r_i(t)$ is convergent to $r^{(i-1)}(t)$, $i \in \{1, 2, \cdots, n\}$ must be ensured.

3. The proposed Generalized Tracking Differentiator (GTD)

The proposed nonlinear tracking differentiator is illustrated in this section. Firstly, an n-th order generalized model for the tracking differentiator based on sigmoid function is presented and its convergence is proven. Then, a 2nd order version of the proposed tracking differentiator is derived. To investigate the proposed tracking differentiator, a definition of the sigmoid function is presented in the following.

Definition 1 (*(Simple sigmoid functions)*). [18]: *A function* $\varphi : \mathbb{R} \to (-1, 1)$ *is supposed to be a sigmoid. The sigmoid function suits the conditions*:

1. The function $\varphi(\cdot)$ is a smooth, i.e., $\varphi(x) \in C^{\infty}$,
2. $\varphi(\cdot)$ is an odd function,
3. the function $\varphi(\cdot)$ satisfies $\lim_{x \to \pm\infty} |\varphi(x)| = 1$.

Since a very large domain is mapped to a small range by the sigmoid function, it is called the "*squashed function*" [18]. A list of sig-

Table 1
List of sigmoid functions.

Sigmoid function	$\varphi(x)$
Hyperbolic tangent function [18,19]	$\tanh(x)$
Elliott squash function [19]	$\frac{x}{1+\lvert x\rvert}$
Specific algebraic function [18]	$\frac{x}{\sqrt{1+x^2}}$
Logistic function [18,20]	$\frac{2}{1+e^{-x}}-1$
Rational functions and absolute value	$\frac{x+2x^3}{1+\lvert x+2x^3\rvert}$

moid functions is given in Table 1 and Fig. 1 illustrates the curve of each function.

The proposed GTDs have the following solid points against other tracking differentiators. These points are listed below:

i. The proposed tracking differentiator is built using a smooth nonlinear function $\varphi(\cdot)$ instead of the *sign*$(\cdot)$ function used in most of the conventional nonlinear differentiators. This is an essential step toward preventing the chattering phenomenon from the output derivatives.
ii. A second improvement is accomplished by combining both the linear and the nonlinear terms. The benefits of this are clear in suppressing high-frequency components in the signal, such as noise. In addition, with this feature, the proposed GTD showed a better performance than those of other tracking differentiators.
iii. The saturation feature of the function $\varphi(\cdot)$ increases the robustness against noisy signals. This is because for large errors, even with a wide range of noise, it is mapped to a small domain set of the function $\varphi(\cdot)$.
iv. Increasing the slope of the continuous function $\varphi(\cdot)$ near the origin significantly accelerates the convergence of the proposed tracking differentiator.

Assumption A1:. *The function* φ *in* Definition 1 *is an odd function with*

$$\psi(y)=\int_0^y \varphi(u)du \geq 0$$

Assumption A2:. *There exists an asymptotically stable linear dynamics given below,*

$$\begin{cases} \dot{z}_1(\tau)=z_2(\tau), \\ \vdots \\ \dot{z}_i(\tau)=z_{i+1}(\tau), \\ \vdots \\ \dot{z}_n(\tau)=-a_1z_1(\tau)-a_2z_2(\tau)-\cdots-a_nz_n(\tau). \end{cases} \tag{2}$$

$a_i>0, i=\{1,2,\cdots,n\}$

The system given in (2) can be symbolized, i.e., $\dot{z}=Az$, where A is a Hurwitz (stable) matrix given by

$$\boldsymbol{A}=\begin{pmatrix} 0 & 1 & 0 & & \cdots & 0 & 0 \\ 0 & 0 & 1 & & \cdots & 0 & 0 \\ \vdots & \vdots & \vdots & & \ddots & \vdots & \vdots \\ 0 & 0 & 0 & \cdots & 1 & 0 & \\ 0 & 0 & 0 & \cdots & 0 & 1 & \\ -a_1 & -a_2 & -a_3 & \cdots & -a_{n-1} & -a_n & \end{pmatrix} \tag{3}$$

Every root of the characteristic polynomial given by $|\lambda \boldsymbol{I}-\boldsymbol{A}|=0$ has a negative real part.

Assumption A3:. $V:\mathbb{R}^n\to\mathbb{R}^+$ *and* $W:\mathbb{R}^n\to\mathbb{R}^+$ *are candidate Lyapunov functions that are continuously differentiable,* $V(z)$ *is extant along with the solution of* (2) *with* $\left|\frac{\partial V}{\partial z_i}\right|<M, i\in\{1,2,\cdots,n\}$ *and* $\dot{V}=-W$.

Theorem 1 (*(nth order GTD):*). *If the signal* $r(t)$ *is differentiable and* $t\in[0,\infty)\sup\left|r^{(n-1)}(t)\right|\leq B$

Then, the differentiator described by,

$$\begin{cases} \dot{r}_1(t)=r_2(t), r_1(0)=r_{10} \\ \dot{r}_2(t)=r_3(t), r_2(0)=r_{20} \\ \vdots \\ \dot{r}_n(t)=-a_1R^n\varphi(r_1(t)-r(t)) \\ -a_2R^{n-1}r_2(t)-\cdots-a_nRr_n(t), r_n(0)=r_{n0} \end{cases} \tag{4}$$

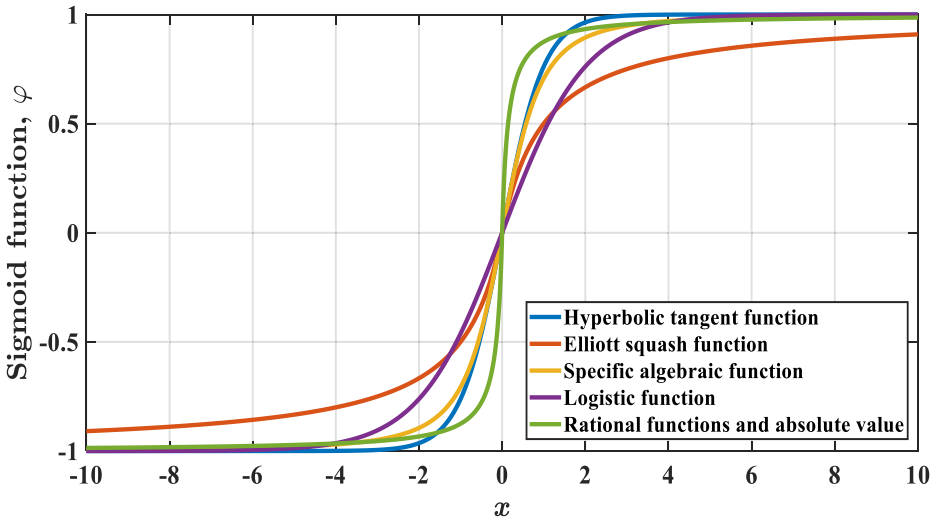

Fig. 1. Some selected sigmoid functions.

is convergent in the sense that, $r_1(t)$ is convergent to $r(t)$ as $R \to \infty$.

Proof:. *Assume,* $t = \frac{\tau}{R}$. *Then*

$\dot{r}_i(t) = \frac{dr_i(t)}{d\tau}\frac{d\tau}{dt} = R\frac{dr_i(t)}{d\tau}$ for $i \in \{1, 2, \cdots, n\}$. (5)

Combining (4) and (5) yields

$$\begin{cases} R\frac{dr_1(\frac{\tau}{R})}{d\tau} = r_2(\frac{\tau}{R}) \\ R\frac{dr_2(\frac{\tau}{R})}{d\tau} = r_3(\frac{\tau}{R}) \\ \vdots \\ R\frac{dr_n(\frac{\tau}{R})}{d\tau} = -a_1R^n\varphi(r_1(\frac{\tau}{R}) - r(\frac{\tau}{R})) \\ -a_2R^{n-1}r_2(\frac{\tau}{R}) - \cdots - a_nRr_n(\frac{\tau}{R}) \end{cases} \tag{6}$$

Then,

$$\begin{cases} \frac{dr_1(\frac{\tau}{R})}{d\tau} = \frac{1}{R}r_2(\frac{\tau}{R}) \\ \frac{dr_2(\frac{\tau}{R})}{d\tau} = \frac{1}{R}r_3(\frac{\tau}{R}) \\ \vdots \\ \frac{dr_n(\frac{\tau}{R})}{d\tau} = -a_1R^{n-1}\varphi(r_1(\frac{\tau}{R}) - r(\frac{\tau}{R})) \\ -a_2R^{n-2}r_2(\frac{\tau}{R}) - \cdots - a_nr_n(\frac{\tau}{R}) \end{cases} \tag{7}$$

Let,

$$\begin{cases} z_1(\tau) = r_1(\frac{\tau}{R}) - r(\frac{\tau}{R}), \\ z_i(\tau) = \frac{1}{R^{i-1}}r_i(\frac{\tau}{R}), i \in \{2, 3, \cdots, n\}. \end{cases} \tag{8}$$

It follows that,

$$\begin{cases} \frac{dz_1(\tau)}{d\tau} = \frac{dr_1(\frac{\tau}{R})}{d\tau} - \frac{dr(\frac{\tau}{R})}{d\tau} \\ \frac{dz_i(\tau)}{d\tau} = \frac{1}{R^{i-1}}\frac{dr_i(\frac{\tau}{R})}{d\tau}, i \in \{2, 3, \cdots, n\}. \end{cases} \tag{9}$$

This together with (9) gives,

$$\begin{cases} \frac{dz_1(\tau)}{d\tau} = \frac{1}{R}r_2(\frac{\tau}{R}) - \frac{dr(\frac{\tau}{R})}{d\tau} \\ \frac{dz_2(\tau)}{d\tau} = \frac{1}{R^2}r_3(\frac{\tau}{R}) \\ \vdots \\ \frac{dz_n(\tau)}{d\tau} = \frac{1}{R^{n-1}}\left[-a_1R^{n-1}\varphi(r_1(\frac{\tau}{R}) - r(\frac{\tau}{R})) - a_2R^{n-2}r_2(\frac{\tau}{R}) \cdots - a_nr_n(\frac{\tau}{R})\right] \end{cases} \tag{10}$$

This results in,

$$\begin{cases} \dot{z}_1(\tau) = \frac{1}{R}r_2(\frac{\tau}{R}) - \frac{dr(\frac{\tau}{R})}{d\tau} \\ \dot{z}_2(\tau) = \frac{1}{R^2}r_3(\frac{\tau}{R}) \\ \vdots \\ \dot{z}_n(\tau) = -a_1\varphi(r_1(\frac{\tau}{R}) - r(\frac{\tau}{R})) \\ -a_2R^{-1}r_2(\frac{\tau}{R}) - \cdots - a_n\frac{1}{R^{n-1}}r_n(\frac{\tau}{R}). \end{cases} \tag{11}$$

substituting (8) in (11) gives

$$\begin{cases} \dot{z}_1(\tau) = z_2(\tau) - \frac{dr(\frac{\tau}{R})}{d\tau} \\ \dot{z}_2(\tau) = z_3(\tau) \\ \vdots \\ \dot{z}_n(\tau) = -a_1\varphi(z_1(\tau)) - a_2z_2(\tau) - \cdots - a_nz_n(\tau). \end{cases} \tag{12}$$

Select the candidate Lyapunov function $V(z)$ based on Assumption A3. Then,

$$\dot{V}\Big|_{along(12)} = \sum_{i=1}^{n}\frac{\partial V}{\partial z_i}\dot{z}_i$$

$$= \sum_{i=1}^{n-1}\frac{\partial V}{\partial z_i}z_{i+1} - \frac{\partial V}{\partial z_1}\frac{dr(\frac{\tau}{R})}{d\tau} + \frac{\partial V}{\partial z_n}(-a_1\varphi(z_1(\tau)) - a_2z_2(\tau) - \cdots - a_nz_n(\tau)) \tag{13}$$

It follows that,

$$\dot{V} = \sum_{i=1}^{n-1}\frac{\partial V}{\partial z_i}z_{i+1} + \frac{\partial V}{\partial z_n}(-a_1z_1(\tau) - a_2z_2(\tau) - \cdots - a_nz_n(\tau)) - a_1\frac{\partial V}{\partial z_n}\varphi(z_1(\tau)) + a_1\frac{\partial V}{\partial z_n}z_1(\tau) - \frac{\partial V}{\partial z_1}\frac{dr(\frac{\tau}{R})}{d\tau} \tag{14}$$

From Assumptions A2 and A 3, we have,

$$\dot{V} = -W - a_1\frac{\partial V}{\partial z_n}(\varphi(z_1(\tau)) - z_1(\tau)) - \frac{\partial V}{\partial z_1}\dot{r}(t)\frac{1}{R} \tag{15}$$

Then,

$$\dot{V} \le a_1M|\varphi(z_1(\tau)) - z_1(\tau)| + \frac{MB}{R} \tag{16}$$

For small values of a_1 around zero and large value of R in the above equation, we obtain

$$\lim_{R\to\infty a_1\to 0}\dot{V}(z) \le 0. \tag{17}$$

Then the solution of (12) is Globally Asymptotically Stable (GAS) based on LaSalle's Invariance principle [21]. It follows that $\lim_{R\to\infty} z_1 = 0$. From (8) we get

$$\lim_{R\to\infty} r_1 = r \tag{18}$$

A 2nd order Generalized Tracking Differentiator (2nd GTD) can be deduced from (4) as follows,

$$\begin{cases} \dot{r}_1(t) = r_2(t), \\ \dot{r}_2(t) = -R^2\varphi(r_1(t) - r(t)) - Rr_2(t). \end{cases} \tag{19}$$

A 2nd order Improved Generalized Tracking Differentiator (IGTD) is constructed from (19) by letting the function φ in Definition 1 is expressed as $\varphi(r_1, r, \alpha, \beta, \gamma) = tanh\left(\frac{\beta r_1 - (1-\alpha)r}{\gamma}\right)$, $a_1 = a_2 = 1$. Then the 2nd order IGTD is given as

$$\begin{cases} \dot{r}_1 = r_2 \\ \dot{r}_2 = -R^2\tanh\left(\frac{\beta r_1 - (1-\alpha)r}{\gamma}\right) - Rr_2 \end{cases} \tag{20}$$

where r_1 tracks the input r, and r_2 tracks the differentiation of input v. The coefficients α, β, γ, are appropriate design parameters added to improve the performance of the original GTD, where $0 < \alpha < 1, \beta > 0$, $\gamma > 0$, and $R > 0$.

Remark 1:. *The improvements added to (19) to obtain the IGTD of (20) are presented and discussed in a conference paper [22], where the convergence and the stability analysis of such improvements are analyzed in detail. In the next, we will investigate the effectiveness of the proposed 2nd order IGTD.*

4. Numerical example

4.1. Numerical results

Some numerical simulations are demonstrated in this section using the second-order IGTD expressed as,

$$\begin{cases} \dot{r}_1 = r_2 \\ \dot{r}_2 = -a_1R^2tanh\left(\frac{\beta r_1 - (1-\alpha)r}{\gamma}\right) - a_2Rr_2 \end{cases} \tag{21}$$

The numerical simulations are implemented under MATLAB environment with 4th order Runge-Kutta method and a step size of 2×10^{-3} . It was considered that $t_0 = 0, t_f = 2sec$, and $\boldsymbol{r}(0) = 0$. These simulations involve a comparison of the offered second-order IGTD given by (21) with the REUCAOD [8] given in Appendix A. The second-order IGTD was tested using the signal $sin(2\pi t) + \mathcal{N}(t)$ as the input signal $r(t)$, an analog signal that is planned to be calculated in a continuous fashion. While the noise component $\mathcal{N}(t)$ adopted in this work as a sinusoidal function with the next two cases:

1. Low-frequency noise component with an amplitude of 0.001, $\mathcal{N}(t) = 0.001 \sin(2\pi \times 10t)$.
2. High-frequency noise component with an amplitude of 0.1, $\mathcal{N}(t) = 0.1 \sin(2\pi \times 100t)$.

The performance indices that are utilized in this work to demonstrate the performance of the second-order IGTD are explained as [23]:

1. Integral Absolute Error (IAE)

$$\text{IAE} = \int_0^{t_f} |e(t)|dt$$

2. Mean Square Error (MSE)

$$\text{MSE} = \frac{1}{t_f} \int_0^{t_f} e(t)^2 dt$$

3. Integral time Square error (ITSE)

$\text{ITSE} = \int_0^{t_f} te(t)^2 dt$, and

4. Integral Time Absolute Error (ITAE)

$$\text{ITAE} = \int_0^{t_f} t|e(t)|dt$$

where $e(t) = 2\pi \cos(2\pi t) - z_2$ is the estimation error for the derivative. The set of parameters for each tracking differentiator used in the comparison in addition to our proposed 2nd order IGTD are listed in Table 2. For the first case, with $r(t) = \sin(2\pi t) + 0.001 \sin(2\pi \times 10t))$, the results of the tracking differentiator used in the comparison are shown in Fig. 2, while Fig. 3 shows the result for the proposed 2nd order IGTD. The aforementioned performance indices are calculated for these tracking differentiators including our proposed 2nd order IGTD and they are presented in Table 3. The tuning process of the IGTD units and the conventional differentiator has been accomplished using a Genetic Algorithm (GA) under a MATLAB environment, minimizing the aforementioned performance indices.

It can be seen from simulations that the proposed 2nd-IGTD presented an accurate estimation for the input signal and its derivative. While the other tracking differentiator also produced good tracking for the input signal and its derivative, some of them suffered from the peaking phenomenon at the beginning of the simulation time and/or exhibited "*phase lag*" in the tracking due to the integrating action extant in their structures.

Table 2
The tracking differentiators Parameters.

Differentiator	Parameters
REUCAOD	k_1 = 13.3658, k_2 = 221.520, κ_1 = 33.1453, κ_2 = 398.5198, α = 0. 8782, T_u = 0.000089
RCND	ε=0.0017, α = 0.5901,a_{10} = 9.8700, a_{11} = 9.4270, a_{20} = 4.5771, a_{21} = 5.4168
Proposed 2nd order IGTD	α = 0.9176,β = 3.0190,γ = 0.0566,R = 97.9777, a_1 = 2.7962, a_2 = 3.2942

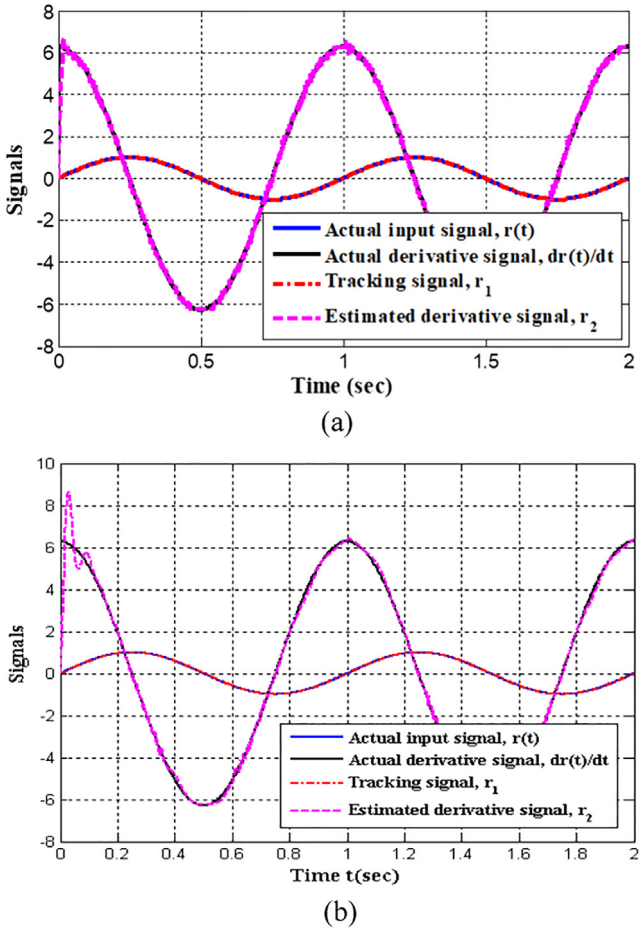

Fig. 2. Tracking input signal $r(t)$ and its 1st derivative using:

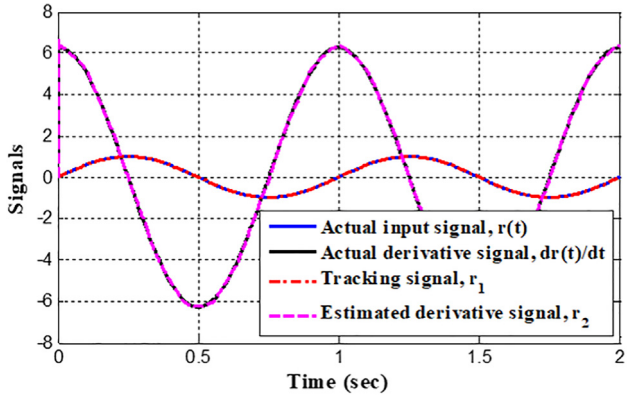

Fig. 3. Tracking input signal $r(t)$ and its 1st derivative using IGTD.

While for the second test with the high-frequency noise component, where $r(t) = \sin(2\pi t) + 0.1 \sin(2\pi \times 100t))$, the bandwidth ω_n is reduced by increasing the value of the γ parameter and reducing the values of both the *R*andβ parameters. The reason for this reduction will be explained immediately following the simulation results. The new parameters of the proposed 2nd-IGTD in this test are selected as $\beta = 1.8228$, $\gamma = 0.1945$, and $R = 11.7409$. Figs. 4 and 5 present the result of tracking both the suggested $r(t)$ and its 1st derivative. As in Table 3, Table 4 shows the enhancement of the proposed 2nd-IGTD performance. Figs. 6 and 7 illustrate the delay associated with both differentiators. It is easy to

Table 3
Performance indices values of case 1.

Tracking Differentiator	MSE	IAE	ITAE	ITSE
REUCAOD	0.10232	0.21279	0.16578	0.02218
RCND	0.02096	0.18175	0.16954	0.02425
IGTD	0.00356	0.08747	0.08489	0.004895

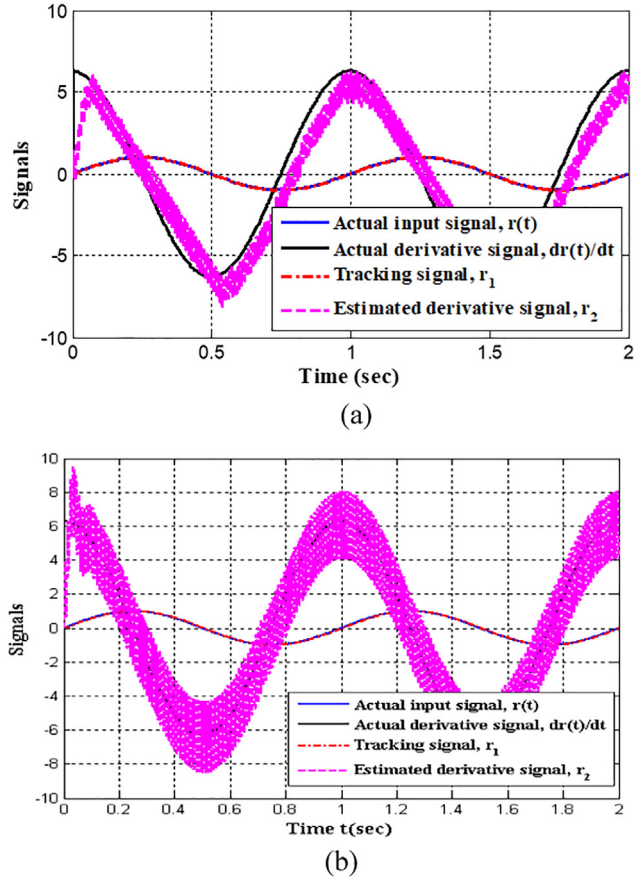

Fig. 4. Tracking input signal $r(t)$ and its 1st derivative in the presence of noise using: (a) REUCAOD (b) RCND.

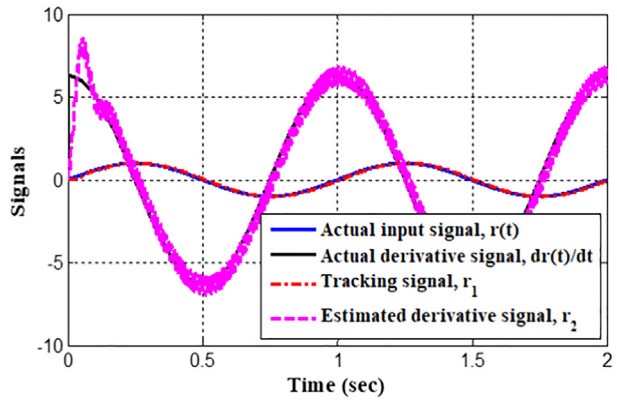

Fig. 5. Tracking input signal $r(t)$ and its 1st derivative in the presence of noise using IGTD.

notice the relatively large delay associated with the REUCAOD tracking differentiator (see Fig. 6) concerning the negligible delay (delay-free) for the IGTD (see Fig. 7).

More numerical simulations are demonstrated in this section using the 3rd-order IGTD whicxh is expressed as,

$$\begin{cases} \overset{\dot{r}_1=r_2}{\dot{r}_2=r_3} \\ \dot{r}_3 = -a_1R^3 tanh\left(\frac{\beta r_1-(1-\alpha)r}{\gamma}\right) - a_2R^2r_2 - a_3Rr_3 \end{cases} \tag{22}$$

The results of these simulations are shown in Fig. 8.

It is clear from Table 3 that the proposed 2nd-IGTD showed a big reduction in the four performance indices. The presence of noise in the input signal had a minimum effect on the estimated derivative of the input signal. This case is reflected in the results listed in Table 4. The proposed 2nd-IGTD proved superior to the REUCAOD tracking differentiator by solving the common issues already extant in the conventional differentiators. One of these issues is the "*peaking phenomenon*". This phenomenon is reduced by considering the proposed 2nd-IGTD of (21) with an optimized set of parameters, a_1, and a_2. Besides, the proposed 2nd-IGTD eliminated the "*phase lag*" problem that is extant in most of the conventional tracking differentiators. This is due to the scaling parameters α and β. The input scaling parameter α reduces the values of the input signal $r(t)$ level by (1- α), while the scaling parameter β amplifies the level of the output signal $r_1(t)$, and thus accelerates the tracking phase. Finally, for signals contaminated with "noise $\mathcal{N}(t)$ ", it is clear that as the frequency of the noise component $\mathcal{N}(t)$ increases regardless of the amplitude level of $\mathcal{N}(t)$, the proposed 2nd-IGTD shows a significant performance improvement. This improvement is due to the reduction in the bandwidth ω_n of the 2nd-IGTD, and since the frequencies of the noise are much higher than ω_n , this makes the proposed 2nd-IGTD act as a band-limiting attenuator to $\mathcal{N}(t)$. The 3rd IGTD presented in Fig. 8 shows a highly accurate estimation of the 2nd order derivative, this is done by expanding the 2nd IGTD by adding an additional state to the differentiator.

4.2. Discussion

The proposed GTDs have the following solid points against other tracking differentiators. The proposed tracking differentiator is built using a smooth nonlinear function $\varphi(\cdot)$ instead of the sign$(\cdot)$ function used in most of the conventional nonlinear TDs. This is an essential step toward preventing the chattering phenomenon from the output derivatives. A second improvement is accomplished by combining both the linear and nonlinear terms. The benefits of this are clear in suppressing high-frequency components in the signal, such as noise. Also, with this feature, the proposed GTD showed a better performance than that of the REUCAOD tracking differentiator. The saturation feature of the function $\varphi(\cdot)$ increases the robustness against noisy signals. This is because for large errors, even with a wide range of noise, it is mapped to a small domain set of the function $\varphi(\cdot)$. Large values of the function's slope around the origin substantially speed up the proposed IGTD on the account of the chattering phenomenon in the differentiator's output profile. Finally, the proposed GTD can be used in feedback control systems and integrated with one of the control design methods like [24–35].

Table 4
Performance indices values of case 2.

Differentiator	MSE	IAE	ITAE	ITSE
REUCAOD	2.18345	2.44571	2.45583	3.96309
RCND	161.3472	23.5615	23.5686	322.8788
IGTD	0.56481	1.00870	0.85090	0.53201

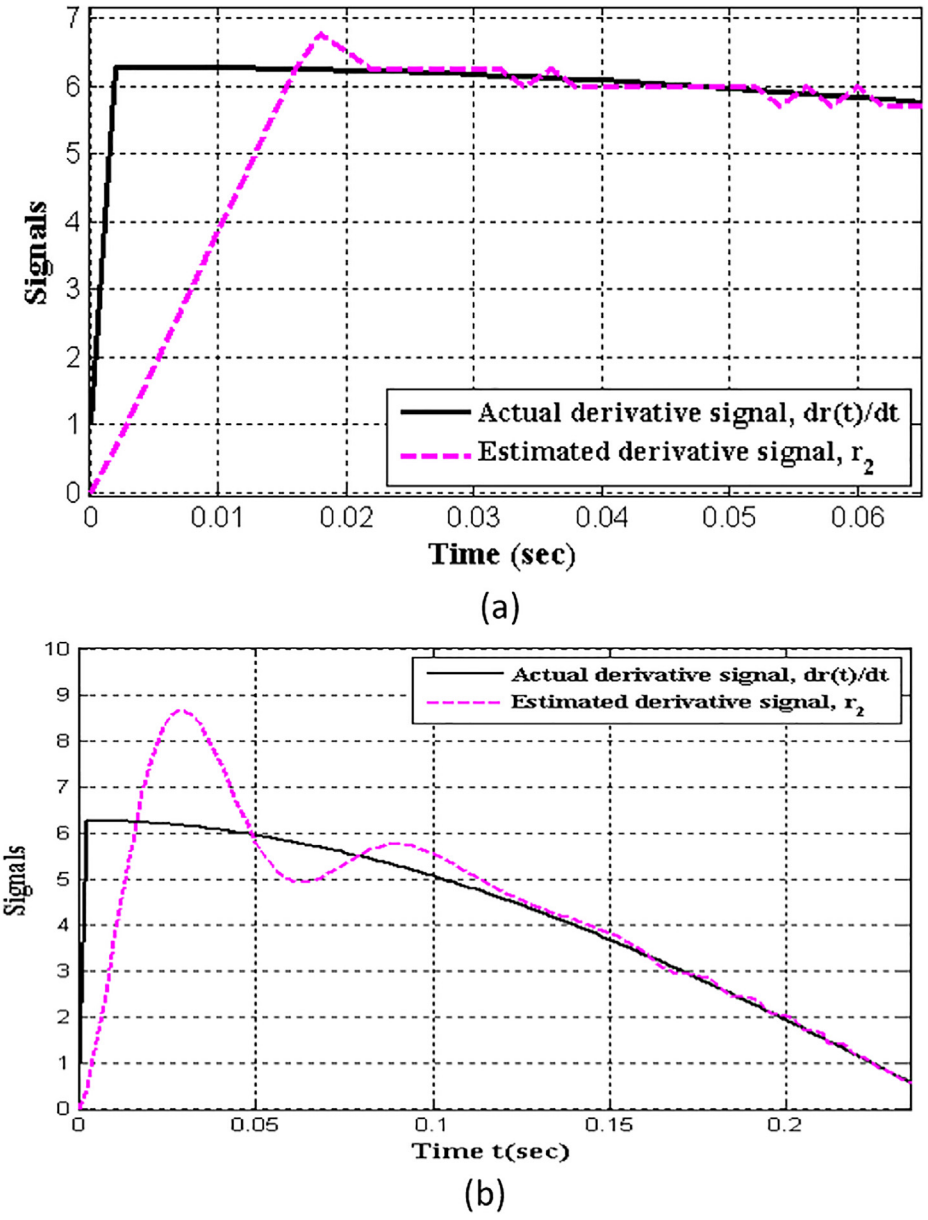

Fig. 6. Actual derivative signal $r(t)$ and its Estimated 1st derivative using: (a) REUCAOD (b) RCND.

5. Conclusion

A GTD is developed based on the sigmoid function to generate a smooth reference signal profile (i.e., the signal itself and its (n-1) derivatives). It encompasses a continuous structure with linear and nonlinear parts and offers an accurate tracking and high robustness against measurement noise which satisfies the high requirements for the underlying applications. The proposed GTD is proven to be globally asymptotically stable and accomplishes smooth and fast-tracking to the input signal and its derivatives. Some improvements have been added to a 2nd order version of the proposed GTD and the simulations showed that the improved differentiator, namely, 2nd-IGTD considerably diminishes "peaking phenomenon" and "noise" and totally eliminates the "chattering phenomenon" from the signal profile and presents better results as compared to REUCAOD one in terms of MSE, ITAE, IAE, ITSE performance time-domain measures. Finally, since the proposed IGTD is a system of nonlinear ordinary differential equations (ODEs), then, as a future work, it can be accurately solved by a numeric-analytic approach, i.e., the Adomian Decomposition Method

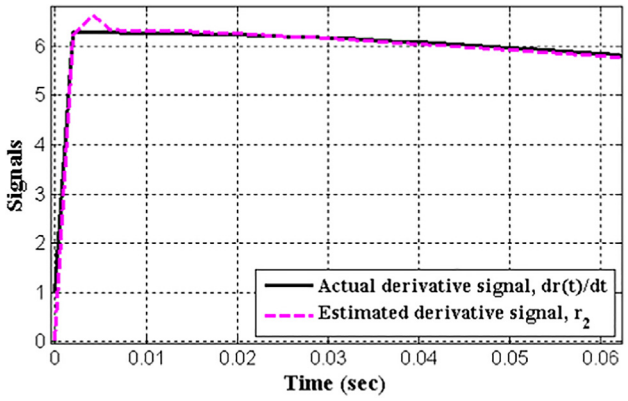

Fig. 7. Actual derivative signal $r(t)$ and its Estimated 1st derivative using IGTD.

(ADM) and its variant, namely, the multistage ADM as explained in [36–38].

Declaration of Competing Interest

The authors declare that they have no known competing financial interests or personal relationships that could have appeared to influence the work reported in this paper.

Appendix A

A.1 *Robust exact uniformly convergent arbitrary order differentiator (REUCAOD)*

The REUCAOD originated from the high order sliding mode differentiator. It was developed in [8] as follows:

$$\begin{cases} \dot{r}_1 = r_2 - \kappa_1\theta|r_1 - r|^{\frac{1}{2}}sgn(r_1 - r) \\ -K_1(1-\theta)|r_1 0 - r|^{\frac{2+\alpha}{2}}sgn(r_1 - r) \\ \dot{r}_2 = -\kappa_2\theta sgn(r_1 - r) - K_2(1-\theta)|r_1 - r|^{1+\alpha}sgn(r_1 - r) \end{cases} \quad (A.1)$$

where $\kappa_1, \kappa_2, k_1, k_2, \theta,$ andα are appropriate design parameters. The differentiator is uniformly finite-time exact when its parameters are selected as follows:

(i) $\{\kappa_i\}_{i=1}^{n}$ are selected based on the bound L of the n-th derivative of the signal using the formulas in [39].

(ii) $\alpha > 0$ is chosen small enough and $\{K_i\}_{i=1}^{n}$ are selected such that the following matrix is Hurwitz:

$$A = \begin{pmatrix} -K_1 & 1 & 0\cdots 0 \\ -K_2 & 0 & 1\cdots 0 \\ \vdots & \vdots & \vdots \\ -K_n & 0 & \cdots 00 \end{pmatrix} \quad (A.2)$$

(iii) the function $\theta : [0, \infty) \rightarrow \{0,1\}$ is selected as

$$\theta(t) = \begin{cases} 0 if t \le T_u \\ 1 otherwise \end{cases} \quad (A.3)$$

With some arbitrary chosen $T_u > 0$

A.2 Rapid Convergent Nonlinear Differentiator (RCND)

The RCND improved the dynamic performance effectively. Also, high-frequency noise can be suppressed sufficiently. The chattering phenomenon can be prevented in the output of the derivative estimation. Moreover, a degree of high robustness is obtained by integrating sliding mode terms and a linear filter. Finally, the differentiator is not appropriate for delayed signals. The RCND can be formulated in the following state-space representation [7]:

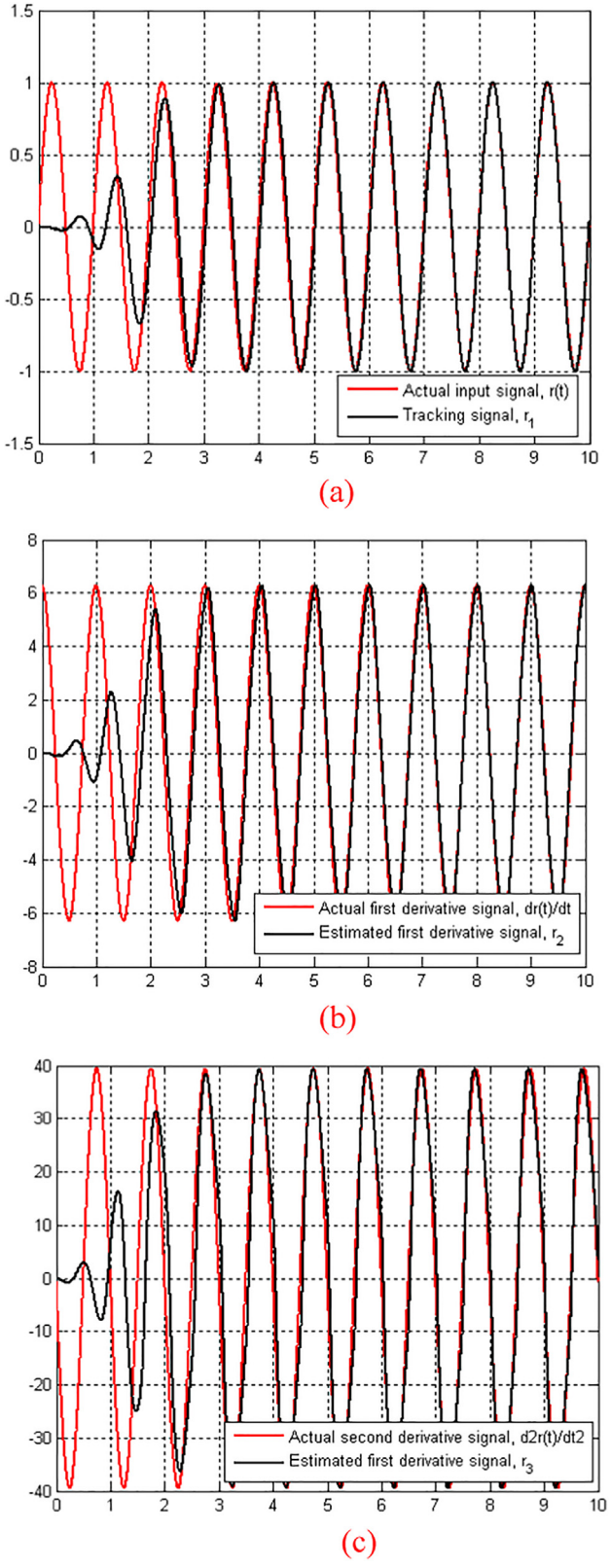

Fig. 8. Response of the 3rd-order IGTD, (a) Input signal $r(t)$ and its Estimation using IGTD,(b) Actual 1st derivative signal $r(t)$ and its Estimated 1st derivative using IGTD, (c) Actual 2nd derivative signal $r(t)$ and its Estimated 2nd derivative using IGTD.

$$\begin{cases} \dot{r}_1 = r_2, \\ \varepsilon^2 \dot{r}_2 = -a_{10}(r_1 - r) - a_{11} sig(r_1 - r)^{\frac{\alpha}{2-\alpha}} - a_{20}\varepsilon r_2 - a_{21} sig(\varepsilon r_2)^{\alpha}. \end{cases} \tag{B.1}$$

Where $\alpha \in (0,1)$ is the perturbation parameter, $a_{10}, a_{11}, a_{20}, and a_{21}$ are positive constants, and $sig(y) = |y|^{\alpha} sgn(y), \alpha > 0$.

References

[1] Vasiljevic LK, Khalil HK. Differentiation with High-Gain Observers the Presence of Measurement Noise. 45th IEEE Conf. Decis. Control, San Diego, CA, USA, 2006, pp. 4717–22. doi:10.1109/CDC.2006.377230.

[2] Levant A. Robust exact differentiation via sliding mode technique. Automatica 1998;34(3):379–84. doi: https://doi.org/10.1016/S0005-1098(97)00209-4.

[3] Hongwei W, Heping W. A Comparison Study of Advanced Tracking Differentiator Design Techniques. Procedia Eng 2015;99:1005–13. doi: https://doi.org/10.1016/j.proeng.2014.12.634.

[4] Khalil HK. Robust servomechanism output feedback controllers for feedback linearizable systems. Automatica 1994;30(10):1587–99. doi: https://doi.org/10.1016/0005-1098(94)90098-1.

[5] Dabroom AM, Khalil HK. Discrete-time implementation of high-gain observers for numerical differentiation. Int J Control 1999;72(17):1523–37. doi: https://doi.org/10.1080/002071799220029.

[6] Lin H, Wang X. Design and analysis of a continuous hybrid differentiator. IET Control Theory Appl 2011;5(11):1321–34. doi: https://doi.org/10.1049/iet-cta.2010.0330.

[7] Wang X, Shirinzadeh B. Rapid-convergent nonlinear differentiator. Mech Syst Signal Process 2012;28:414–31. doi: https://doi.org/10.1016/j.ymssp.2011.09.026.

[8] Angulo MT, Moreno JA, Fridman L. Robust exact uniformly convergent arbitrary order differentiator. Automatica 2013;49(8):2489–95. doi: https://doi.org/10.1016/j.automatica.2013.04.034.

[9] Shen Y, Shao K, Ren W, Liu Y. Diving control of Autonomous Underwater Vehicle based on improved active disturbance rejection control approach. Neurocomputing 2016;173(3):1377–85. doi: https://doi.org/10.1016/j.neucom.2015.09.010.

[10] Shi G, Zong X, Cheng X. An improved detecting approach of harmonic current in single-phase active power filter based on tracking differentiator. Proc. 6th Int. Conf. Intell. Control Inf. Process. ICICIP, Wuhan, China 2015, pp. 343-347, doi:10.1109/ICICIP.2015.7388194.

[11] Yu H, Wang H. Application of tracking-differentiator in angular measurements on spinning projectiles using magnetic sensors. 7th Int. Conf. Intell. Human-Machine Syst. Cybern. IHMSC, Hangzhou, China, 2015, pp. 433-436, doi:10.1109/IHMSC.2015.25.

[12] Abdul-adheem WR, Ibraheem IK. Improved Sliding Mode Nonlinear Extended State Observer based Active Disturbance Rejection Control for Uncertain Systems with Unknown Total Disturbance. Int J Adv Comput Sci Appl 2016;7(12):80–93. doi: https://doi.org/10.14569/IJACSA.2016.071211.

[13] Abdul-adheem WR, Ibraheem IK arxiv.org/abs/1805.12170. An Improved Active Disturbance Rejection Control for a Differential Drive Mobile Robot with Mismatched Disturbances and Uncertainties 2018.

[14] Ibraheem IK. Anti-disturbance compensator design for unmanned aerial vehicle. J Eng 2020;26(1):86–103.

[15] Cheng Y, Chen Z, Sun M, Sun Q. Decoupling control of a binary distillation column with measurement noise. Chinese Control Conf CCC 2018;2018-July:2741–6.

[16] Shao Xingling, Liu Jun, Yang Wei, Tang Jun, Li Jie. Augmented nonlinear differentiator design. Mech Syst Sig Process 2017;90:268–84.

[17] Park Jang-Hyun, Kim Seong-Hwan, Park Tae-Sik. Asymptotically convergent switching differentiator. Int J Adapt Control Signal Process 2019;33(3):557–66.

[18] Menon A, Mehrotra K, Mohan CK, Ranka S. Characterization of a class of sigmoid functions with applications to neural networks. Neural Networks 1996;9(5):819–35. doi: https://doi.org/10.1016/0893-60809(5)00107-7.

[19] D. L. Elliott, "A Better Activation Function for Artificial Neural Network," Report, the Institute for Systems Research (ISR) - University of Maryland, TR 93-8, January 29, 1993.

[20] Jang DW, Park RH. Color fringe correction by the color difference prediction using the logistic function. IEEE Trans Image Process 2017;26(5):2561–70. doi: https://doi.org/10.1109/TIP.2017.2687125.

[21] Khalil HK, Nonlinear Systems. New Jersey: Prentice-Hall, 1996.

[22] Ibraheem IK, Abdul-Adheem WR. A novel second-order nonlinear differentiator with application to active disturbance rejection control. 1st International Scientific Conference of Engineering Sciences - 3rd Scientific Conference of Engineering Science (ISCES), Diyala, Iraq, 2018, pp. 68 - 73, doi: 10.1109/ISCES.2018.8340530.

[23] Dorf RC, Bishop RH. Modern control systems. 12th ed. Pearson Education; 2011.

[24] Ibraheem IK. On the frequency domain solution of the speed governor design of non-minimum phase hydro power plant. Mediterr J Meas Control 2012;8(3):422–9.

[25] Mohammed IA, Maher RA, Ibraheem IK. Robust controller design for load frequency control in power systems using state-space approach. J Eng 2011;17(3):265–78.

[26] Tuaimah, F.M.; Ibraheem, I.K. (2010). Robust H_∞ Controller Design for Hydro Turbines Governor, 2nd Regional Conf. for Eng.Sciences/ College of Eng./ Al-Nahrain University, Baghdad, Iraq, 1-9.

[27] Maher Rami A, Mohammed Ismail A, Ibraheem Ibraheem Kasim. Polynomial based H_∞ robust governor for load frequency control in steam turbine power systems. Int J Electr Power Energy Syst 2014;57:311–7.

[28] Al-Qassar AA, Abdulkareem AI, Humaidi AJ, Ibraheem IK, Azar AT, Hameed AH. Grey-wolf optimization better enhances the dynamic performance of roll motion for tail-sitter VTOL aircraft guided and controlled by STSMC. J Eng Sci Technol 2021;16(3):1932–50.

[29] Al-Qassar, A.A.; AL-Dujaili, A.Q.; HASAN, A.F.; Humaidi, A.J.; Ibraheem, I.K.; Azar, A.T.(2021). Stabilization Of Single-Axis Propeller-Powered System For Aircraft Applications Based On Optimal Adaptive Control Design, 16(3), 1851-1869.

[30] Ajel AR, Humaidi AJ, Ibraheem IK, Azar AT. Robust model reference adaptive control for tail-sitter VTOL aircraft. Actuators (MDPI) 2021;10(7):162.

[31] Ibraheem IK. A digital-based optimal AVR design of synchronous generator exciter using LQR technique. Al-Khwarizmi Eng J 2011;7(1):82–94.

[32] Ibraheem IK. Damping low frequency oscillations in power system using quadratic gaussian technique based control system design. Int J Comput Appl 2014;92(11):18–23.

[33] Maher Rami A, Mohammed Ismail A, Ibraheem Ibraheem Kasim. State-space based H_∞ robust controller design for boiler-turbine system. Arab J Sci Eng 2012;37(6):1767–76.

[34] Ibraheem, I.K. (2009). Robust governor design for hydro machines using H_∞ loop-shaping techniques, Proceedings of the 6th Engineering Conference, Baghdad, Iraq, 4, 403-414.

[35] Hadi, N.H., Ibraheem, I.K. (2021). Speed control of an SPMSM using a tracking differentiator-PID controller scheme with a genetic algorithm, International Journal of Electrical and Computer Engineering, 11(2), 1728-1741.

[36] Fatoorehchi H, Alidadi M, Rach R, Shojaeian A. Theoretical and experimental investigation of thermal dynamics of steinhart-hart negative temperature coefficient thermistors. J Heat Transfer 2019;141:1–11.

[37] Fatoorehchi Hooman, Abolghasemi Hossein, Zarghami Reza, Rach Randolph. Feedback control strategies for a cerium-catalyzed Belousov-Zhabotinsky chemical reaction system. Can J Chem Eng 2015;93(7):1212–21.

[38] Duan Nan, Sun Kai. Power System Simulation Using the Multistage Adomian Decomposition Method. IEEE Trans Power Syst 2017;32(1):430–41.

[39] Levant A. Higher-order sliding modes, differentiation and output-feedback control. Int J Control 2003;76(9–10):924–41. doi: https://doi.org/10.1080/0020717031000099029.